Activation of gga-miR-155 by reticuloendotheliosis virus T strain and its contribution to transformation

Activation of gga-miR-155 by reticuloendotheliosis virus T strain and its contribution to transformation

Yongxiu Yao[1*], Deepali Vasoya[2] Lydia Kgosana[1], Lorraine P Smith[1], Yulong Gao[3], Xiaomei Wang[3], Michael Watson[2] and Venugopal Nair[1*]

[1]Avian Viral Disease Programme & UK-China Centre of Excellence on Avian Disease Research, The Pirbright Institute, Pirbright, Ash Road, Guildford, Surrey, United Kingdom GU24 0NF

[2]The Roslin Institute and Royal (Dick) School of Veterinary Studies, University of Edinburgh, Easter Bush, United Kingdom EH25 9RG

[3]Division of Avian Infectious Diseases, State Key Laboratory of Veterinary Biotechnology, Harbin Veterinary Research Institute, Chinese Academy of Agricultural Sciences, Harbin, China

***Corresponding Author**

Tel: +441483 231415

E-mail: venugopal.nair@pirbright.ac.uk; yongxiu.yao@pirbright,ac,uk

Running title: v-*rel* induces gga-miR-155 through the NF-κB pathway

Abstract

The v-*rel* oncoprotein encoded by reticuloendotheliosis virus T strain (Rev-T) is a member of the *rel*/NF-κB family of transcription factors capable of transformation of primary chicken spleen and bone marrow cells. Rapid transformation of avian haematopoietic cells by v-*rel* occurs through a process of deregulation of multiple protein-encoding genes through its direct effect on their promoters. More recently, upregulation of oncogenic miR-155 and its precursor pre-miR-155 were demonstrated in Rev-T-infected chicken embryo fibroblast cultures as well as Rev-T-induced B-cell lymphomas. Through electrophoresis mobility shift assay and reporter analysis on gga-miR-155 promoter, we show that the v-*rel*-induced miR-155 overexpression occurs by the direct binding to one of the putative NF-κB binding sites. Using v-*rel*-induced transformation model on chicken embryonic splenocyte cultures, we could demonstrate dynamic increase in miR-155 levels during the transformation. Transcriptome profiles of lymphoid cells transformed by v-*rel* showed upregulation of miR-155 accompanied by downregulation of a number of putative miR-155 targets such as Pu.1 and CEBPβ. We also show that v-*rel* can rescue the suppression of miR-155 expression observed in Marek's disease virus-transformed cell lines, where its functional viral homolog MDV-miR-M4 is overexpressed. Demonstration of gene expression changes affecting major molecular pathways including organismal injury and cancer in avian macrophages transfected with synthetic mature miR-155 underline its potential direct role in transformation. Our study suggests that v-*rel*-induced transformation involves complex set of events mediated by the direct activation of NF-κB targets together with the inhibitory effects on miRNA targets.

Keywords: v-*rel ,* NF-κB, miR-155, transformation

Introduction

The *rel*/NF-κB family of transcription factors (1, 2) play a key role in the control of cell proliferation and apoptosis, two functions critical in cancer. The involvement of *rel*/NF-κB in malignancy is best demonstrated by the acute oncogenicity of their viral derivative, v-*rel*, first identified in reticuloendotheliosis virus T (Rev-T) strain (3, 4). Rev-T is an acutely transforming variant of REV, the aetiological agent of reticuloendotheliosis in birds, carrying the viral oncogene v-*rel*, a variant of the turkey cellular proto-oncogene c-*rel* (5-7). Because of the rapidity and efficiency of transformation of the cells, the v-*rel* provides a valuable model for studying the role of *rel*/NF-κB family in neoplastic transformation and cancer. The v-*rel*-mediated transformation occurs predominantly through the modulation of transcription of *rel*/NF-κB targets (8-10), the examples of which include AP-1 (11, 12), IRF-4 (13), SH3BGRL (14), TGFβ/Smad (15) and telomerase reverse transcriptase (TERT) subunit (16). More recently, repression of BLNK and BCAP proteins (17) and a novel interaction of CAPERα and the transactivating domain of v-*rel* (18) were shown to be important for lymphocyte transformation by the v-*rel* oncoprotein.

Several studies have also implicated microRNAs (miRNAs) as key mediators of a number of cell regulatory processes including the induction of cancer (19-21). Among the numerous miRNAs expressed in hematopoietic cells, miR-155 was shown to have the most wide ranging effects on the biology of lymphocytes (22-25). It is processed from a primary transcript, known as '*Bic*' (B-cell integration cluster), whose upstream region was originally found to be a frequent site of integration of the avian leukosis virus in lymphomas (26). A number of recent miRNA profiling studies have shown elevated levels of miR-155 in a wide array of cancers including lymphomas (27-30).

In a recent study on chicken embryo fibroblast (CEF) cultures infected with reticuloendotheliosis virus (Rev) HA1101 strain, differential expression of a number of genes

leading to changes in several signalling pathways were reported (31). We and others have shown upregulation of miR-155 in Rev-T-transformed cell lines and CEF (32, 33). For further analysis of the global changes in miRNA profiles induced by v-*rel*, we used an *in vitro* model of v-*rel*-induced transformation of embryonic splenocytes to demonstrate the sequential upregulation of miR-155 during the transformation process. Our studies confirm that v-*rel*-mediated upregulation of gga-miR-155 occurs through the direct binding to at least one of the putative NF-κB sites on the *Bic*/miR-155 promoter. Analysis of the gene expression changes in the v-*rel*-transformed cells further demonstrated downregulation of a number of known miR-155 targets potentially affecting a number of important biological pathways. Demonstration of the targeting of a number of cancer-related genes in chicken macrophages overexpressing miR-155 demonstrated the importance of this miRNA as a major regulator of v-*rel*-induced transformation.

Results

Upregulation of miR-155 in Rev-T transformed cell lines. During the analysis of the global changes in miRNA expression in chicken lymphocyte lines transformed by avian oncogenic viruses, we observed that miR-155 is overexpressed in v-*rel*-transformed chicken lymphocytes, compared to the normal spleen cells and MDV-transformed cell lines (32). For confirmation of the higher expression of miR-155 in v-*rel*-transformed cells, we examined Rev-T-transformed cell lines AVOL-1, AVOL-2, AVOL-3 and RIR-Rev-T cells by Northern blot analysis. An ALV transformed B-cell line HP45 was used as positive control where miR-155 is upregulated due to insertional activation and normal spleen cells which doesn't express detectable levels of miR-155 was used as negative control. High levels of miR-155 transcripts were readily observed in all Rev-T transformed cell lines (Fig 1).

v-*rel* binds to the NF-κB sites in the Bic/miR-155 promoter. Having demonstrated the upregulation of miR-155 in Rev-T transformed cells, we examined the potential mechanisms of miR-155 overexpression by v-*rel*. Analysis of the chicken *Bic*/miR-155 promoter sequence for potential transcription factor binding sites using the program TFSEARCH (34) identified a number of transcription factor binding sites, including two putative NF-κB sites (NF-κB1 & NF-κB2) located at positions -581 and -66 respectively (relative to the transcription start site). In order to establish that v-*rel* binds directly to the putative NF-κB sites in the *Bic*/miR-155 promoter, electrophoresis mobility shift assay was carried out using recombinant GST-v-*rel* fusion protein. Briefly, purified GST-v-*rel* protein was incubated with dsDNA oligonucleotides probe spanning the two putative NF-κB sites. The intense shifted bands were observed with incubation of GST-*v-rel* and wild type labelled probes for both sites (lane 2, Fig 2A). The bands are competed by an excess of cold competitor (lane 3, Fig 2A), but not the same amount of a mutant competitor that is not bound by v-*rel* protein (lane 4, Fig 2A).

NF-κB site 2 in *Bic*/miR-155 promoter is required for miR-155 activation. Having demonstrated the direct binding of v-*rel* to the NF-κB sites, we next examined the possible contribution of these elements in mediating *Bic* regulation. To this end, we carried out reporter assays to examine the ability of v-*rel* to drive the expression of *renilla* luciferase reporter gene using constructs containing the wild type or the mutant chicken *Bic*/miR-155 promoter. For this, the chicken *Bic*/miR-155 promoter region extending from -1829 to +3 nucleotides from transcription start site (+1) was cloned upstream *renilla* luciferase gene of psiCHECK™-2 vector (Promega) to replace the SV40 promoter generating the reporter construct pBic-WT. Mutagenesis of the two NF-κB sites was carried out by overlapping PCR generating pBic-M1, pBic-M2 and pBic-M1M2 constructs, where the NF-κB1, NF-κB2 or both sites respectively, were mutated (Fig 2B). For the reporter assay, each of the reporter and pcDNA3-v-*rel* constructs were co-transfected into DF-1 cells and the luciferase

119 expression was assayed 48 hours later using the Dual-Glo Luciferase Assay System
120 (Promega) following manufacturer's instructions. As shown in Fig 2C, mutation of the first
121 NF-κB site (pBic-M1) did not show obvious changes in the luciferase levels compared to the
122 wild type promoter (pBic-WT) construct. In contrast, mutation of the second NF-κB site
123 (pBic-M2) decreased the promoter activity by 63% compared to that of the pBic-WT,
124 suggesting that the v-*rel*-mediated transactivation occurs mainly through this NF-κB site.
125 The promoter activity of double mutant pBic-M1M2 construct was similar to that of pBic-M2
126 further confirming that the second NF-κB site in the *Bic*/miR-155 promoter is important for
127 the v-*rel*-mediated upregulation of miR-155.

128 **v-*rel* relieves the inhibition of miR-155 expression in MSB-1 cells.** We have previously
129 shown that miR-155 is consistently downregulated in MDV-transformed tumours and cell
130 lines (32). Although the mechanisms for this downregulation are not known, this could be
131 due to the complementation of miR-155 functions by the high levels of the viral homolog
132 MDV-miR-M4 expressed in these cells. We wanted to examine whether the downregulation
133 of miR-155 in MDV transformed cell lines can be rescued by expressing v-*rel* in these cells.
134 RCAS(A)-v-rel-GFP virus stocks were used for transduction of v-*rel* into MSB-1 and 265L,
135 where the GFP marker allowed sorting of the infected cells. Analysis of the sorted cells by
136 Western blotting showed expression of v-*rel*-GFP in both infected MSB-1 and 265L but not
137 in uninfected cells (Fig 3A). Expression of v-*rel* increased the level of miR-155 expression
138 by approximately 700-fold in MSB-1 cells and by about 900-fold in 265L cells which is
139 much higher than the miR-155 level in untransformed CD4+ cells (Fig 3B), demonstrating
140 that ectopic expression of v-rel can induce expression of miR-155 in avian lymphoid cells.

141 **Induction of miR-155 is accompanied by downregulation potential targets.** For further
142 analysis of the dynamic global changes in miRNA profiles during v-*rel*-induced
143 transformation, we examined the changes in RCAS(A)-v-*rel*-infected chicken embryonic

splenocytes undergoing transformation. Induction of v-*rel* in these cells resulted in rapid transformation resulting in the appearance of continuously proliferating cell lines usually in 8-10 days. The dynamic changes of miR-155 expression during the transformation process of splenocytes measured by qRT-PCR are shown in Fig 4A. Quite clearly, miR-155 is significantly upregulated during the time-course of v-*rel* transformation, with levels showing increases of 5 fold (day 1), 6 fold (day 4), 50 fold at day 7, 150 fold at day 9 and nearly 1500 fold at day 14, as compared with the level at day 0.

In order to assess the simultaneous changes in gene expression during transformation, we carried out the transcriptome analysis using the chicken Affymetrix platform on the RNA samples extracted from these cells. To focus on miRNA-induced repression of gene expression, we used the Bioconductor package Limma (35) to extract 1242 genes that showed significant downregulation at day 14 compared to day 0. Table 1 shows the top 20 statistically enriched predicted miRNA targets in this list. Of the 1242 downregulated genes, 73 are predicted targets of gga-miR-155 (Fig 4B) making it the top hit of the most enriched miRNA targets. Analysis also showed that the enrichment of the targets of other miRNAs such as gga-miR-9*, gga-miR-217, gga-miR-19a and gga-miR-23b were also significant. These data highlighted the importance of miR-155 and other miRNAs in *v-rel* induced transformation. MiR-155 is a well-studied oncogene of hematopoietic cells. Considering the complexity of targets analysis in v-*rel* induced transformation system as lots of miRNAs and mRNAs are affected by v-*rel*, we overexpressed miR-155 in chicken macrophages derived from line 0 chicken by transfection of miR-155 mimics into bone-marrow derived macrophages. 'Allstars' negative control (Qiagen) was used as control in an attempt to get a cleaner result on miR-155 targets. The RNA extracted from transfected cells were analysed by deep sequencing. The significant down regulated genes with miR-155 target sites in 3'UTR were subject to the pathway analysis using Ingenuity Pathway Analysis tool. As

shown in Fig 5, several potential miR-155 targets are involved in a number of diseases and cellular processes. The number of cancer-related genes targeted by miR-155 ranks the second implicating the importance of miR-155 as a regulator in disease pathogenesis, particularly in tumorigenesis.

Discussion

The Rev-T avian retrovirus encodes the v-*rel* oncoprotein, which is a member of the Rel/NF-κB transcription factor family. Although Rel/NF-κB transcription factors have been associated with oncogenesis in mammals, v-*rel* is the only member of this family that is oncogenic in animal systems. Due to its pervasive role in oncogenesis, there is great interest in NF-κB signalling, and v-*rel* provides a valuable model for studying NF-κB signalling in lymphoid cell cancers because of its ability to transform chicken lymphoid cells (12, 15). In this study, we demonstrate that v-*rel* can readily induce transformation of lymphocyte populations, and the establishment of CD4+ T-cell (AVOL-1) and B-cell (AVOL-2) lineages suggested that v-*rel*-induced transformation function is not restricted to specific lineages.

In addition to the changes in protein-coding genes, many changes in the miRNA profiles also occur in v-*rel* transformed cells, and one of the miRNAs expressed at significantly higher levels in v-*rel*-derived tumor cell lines such as KBMC and CM758 is gga-miR-155 (33). Higher expression of miR-155 is reported in a number of haematopoietic malignancies (36-40). The precursor of miR-155, termed c-*Bic*, was first observed to co-operate with *myc* in chicken B-cell lymphomas induced by avian leukosis proviral integrations (26, 41). Southern blot hybridization of genomic DNA from AVOL-1 and AVOL-2 cells showed no evidence of genomic rearrangements in *Bic* loci (data not shown) discounting insertional activation of miR-155 in these cell lines. It is known that miR-155 can also be induced by a variety of immune cell stimuli such as TLR ligands, TNF-α, IFN-β and other antigens (41-45). A

194 conserved AP-1 element in the human *Bic*/miR-155 promoter was shown to be essential for
195 some of these functions (46). Transcriptional regulation of miR-155 by TGF-β/Smad4
196 pathway using the Smad response elements in the human miR-155 promoter has also been
197 reported (47). Epstein–Barr virus (EBV) latent membrane protein-1 (LMP1) is a potent
198 inducer of miR-155 and the NF-κB sites in the *Bic*/miR-155 promoter have been shown to be
199 pivotal for this function (48, 49).

200 Both Northern blotting and microarray data showed that miR-155 is significantly increased in
201 v-*rel*-transformed T and B lymphocytes compared to the normal spleen cells. These
202 observations are similar to the findings reported previously (33). Despite the consistent
203 demonstration of transformation of B and T-lymphocytes by v-*rel*, the precise mechanisms
204 have not been demonstrated. As an NF-κB homolog (8), the most likely mechanism of miR-
205 155 upregulation would be through the direct activation of the miR-155 promoter through the
206 NF-κB binding sites. EMSA showed that v-*rel* binds directly to both NF-κB binding sites. To
207 assess the ability of v-*rel* to activate transcription from miR-155 promoter, we performed
208 reporter assays using the miR-155 promoter and its derivative lacking each of the NF-κB
209 binding sites. Our results demonstrated that indeed v-*rel* controls miR-155 through one of the
210 NF-κB binding sites in the *Bic*/miR-155 promoter.

211 A number of previous studies have demonstrated robust expression of *Bic* in EBV-infected
212 cells (50, 51). It has been shown later that EBV-encoded latent membrane protein-1 (LMP-1),
213 a functional homologue of the tumor necrosis factor receptor family, upregulates the
214 expression of miR-155 mainly by activating the NF-κB pathway (48). The data here is the
215 first evidence showing miR-155 being regulated by an NF-κB transcription factor, the v-*rel*
216 oncogene encoded by Rev-T in avian systems. It has been shown previously that v-*rel* exerts
217 downstream effects through the transcription factor AP-1 (12, 46). AP-1 sites are present in

218 chicken *Bic*/miR-155 promoter sequences and the contribution of AP-1 in regulation of miR-
219 155 expression in v-*rel*-transformed lymphocytes remains to be determined.

220 Interestingly, while miR-155 was upregulated in Rev-T transformed cell lines, it was
221 consistently downregulated in MDV-transformed lymphocytes (52). Although miR-155
222 functions are probably rescued by the high level expression of the MDV1-miR-M4 homolog
223 in these cells (53), the precise molecular mechanisms of downregulation of miR-155 in
224 MDV-transformed cells are not clear. RCAS-mediated transduction of v-*rel* did rescue the
225 expression of miR-155 in two of the MDV transformed cell line MSB-1 and 265L. The
226 increased level of miR-155 expression after introduction of v-*rel* into these cells indicated
227 that the upregulation of miR-155 is a direct effect. It is interesting to know that common
228 occurrence of MDV with REV in chickens could lead a part or entire genome of REV
229 integrating into MDV genome (54, 55). Although a number of field MDV isolates with REV
230 insertion have been characterized, the precise molecular mechanisms for the altered
231 pathogenic properties and the increased virulence are still not clear (55, 56).

232 A number of targets of miR-155 have been identified previously. C-Maf (43), AID (57, 58),
233 Pu.1 (59), SOCS1 (60), interleukin-1 (61) and IKKε (49, 62) have been implicated in
234 mediating functions of miR-155 in the immune system. Ets-1 and Meis1 mediate
235 megakaryopoiesis (63). SHIP1 and C/EBP have been implicated in myeloproliferative
236 disorders (64, 65), Peli1 controls the generation and function of T follicular helper cells
237 through promoting the degradation of the NF-κB family transcription factor c-Rel (66), tumor
238 protein p53 inducible nuclear protein 1 (Tp53INP1) is involved in pancreatic cancer (67) and
239 SOCS1 in promoting γ-chain cytokine signalling to ensure effector and memory CD8+ T cell
240 differentiation (68). Additionally, miR-155 targets JARID2, a cell cycle regulator and part of
241 a histone methyltransferase complex, to promote cell survival (33). From microarray data on
242 RNA of v-*rel* transformed cells, 73 out of 1242 significantly downregulated genes are

potential targets of miR-155. Not only was miR-155 the most statistically enriched target within the list of significantly down-regulated genes, but members of the miR-17-92 cluster are also implicated, a cluster which is known to be involved in cancer (69-72), this further emphasized the role of oncogenic miRNAs in transformation.

The oncogenic effects of miR-155 are mediated through its target mRNAs. The known miR-155 targets Pu.1, CEBPβ are present in the down regulated genes from microarray analysis in *v-rel* transformed cells. Together with the evidence that the potential miR-155 targets in macrophages involved in cancer are standing out of other diseases and functions related targets, demonstrating the important role of miR-155 in *v-rel* induced transformation. Although the precise roles and molecular pathways of miR-155 in *v-rel* induced transformation are not fully known, its repressive function on transcriptional factors such as Pu.1 and CEBPβ can have wide-ranging effects on the cellular milieu and the global gene expression profiles seen for lymphocytes. Further studies will be required to ascertain the involvement of Pu.1, CEBPβ and/or other miR-155 regulated transcription factors in the regulation of miR-155-inhibited genes. Similarly, the repression of some of the other target genes is also likely to contribute to the induction of hematopoietic cell malignancy. Although upregulation of miR-155 appears to add complexity to regulation of gene expression in v-*rel*–induced malignant transformation, the downstream network of miR-155 targets or the importance of those target genes in v-*rel* induced transformation could be an interesting area to explore.

Materials and methods

Transformed cell lines

Rev-T-transformed cell lines AVOL-1 ($CD4^+$ T-cell line) (32), AVOL-2 (B-cell origin), AVOL-3, RIR-RevT (a transformed cell line derived from outbred Rhode Island Red chickens) and avian leukosis virus (ALV) HPRS F42 strain-transformed B-cell line HP45 (73) were used. MDV cell lines MSB-1 (74) and 265L (32) were used to study the effects of induction of v-*rel*. All the cell lines were grown at 38.5 °C in 5% CO_2 in RPMI 1640 medium containing 10% fetal calf serum, 2% chicken serum, 10% tryptose phosphate broth, 0.1% 2-mercaptoethanol and 1% sodium pyruvate. CEF-derived cell line DF-1 was grown using methods described (75).

Chicken splenocytes, $CD4^+$ T cells and magnetic cell sorting.

Single-cell suspensions of lymphocytes were prepared from spleen tissues of uninfected birds by using Histopaque-1083 (Sigma-Aldrich) density-gradient centrifugation. $CD4^+$ T cells were isolated by magnetic cell sorting using mouse anti-chicken CD4 antibodies (Chan *et al.*, 1988) and goat anti-mouse IgG microbeads (Miltenyi Biotec). After each antibody treatment, cells were washed three times with PBS containing 0.5% bovine serum albumin. At each wash, the cell suspension was centrifuged at 450 ***g*** for 10 min. Positively stained cells were sorted through an AutoMACS Pro Separator (Miltenyi Biotec). Purity of the sorted cells was confirmed to be >99% by flow cytometry after labelling with monoclonal anti-goat/sheep IgG–fluorescein isothiocyanate (Sigma) antibody (data not shown).

Plasmid constructs

The construct pcDNA3.1-v-*rel* was used for reporter assay. For electrophoresis mobility shift assay, recombinant v-*rel* fused in-frame with GST in pGEX2T (GE Healthcare) vector was used. RCAS(A) retroviral vector (Replication Competent ALV LTR with a Splice acceptor) (76) with v-*rel* cloned into the *Cla*I site was used for *in vitro* transformation of embryonic splenocytes. The orientation of the insert was verified by restriction enzyme digestion and

sequencing. RCAS (A)-EGFP-v-*rel* construct with the N-terminal enhanced green fluorescent protein (EGFP) tag was used for the expression of v-*rel* in MSB-1 and 265L cells.

Cloning and mutagenesis of *Bic*/miR-155 promoter

The chicken *Bic*/miR-155 promoter region extending from -1829 to +3 nucleotides from transcription start site (+1) was amplified by PCR from the genomic DNA prepared from CEF. The isolated fragments were digested with *Bgl*II and *Nhe*I and cloned into *Bgl*II and *Nhe*I cut psiCHECK™-2 vector (Promega) to replace the SV40 promoter driving the *renilla* luciferase gene to generate the pBic-WT reporter construct. Mutagenesis of the two NF-κB sites on the pBic promoter was carried out by overlapping PCR using primers 5′-CCACATATTTCCTTGCTGGCTCGAGACATAAATTTTTCTGAG-3′ and 5′-CTCAGAAAAATTTATGTCTCGAGCCAGCAAGGAAATATGTGG-3′ for NF-κB site 1, 5′-GAAAAGGAAAGCAGGCTCGAGACTCAAGACGGTTAG-3′ and 5′-CTAACCGTCTTGAGTCTCGAGCCTGCTTTCCTTTTC-3′ for NF-κB site 2. The mutant constructs were used to replace the corresponding fragment in the pBic-WT vector to generate pBic-M1, pBic-M2 and pBic-M1M2 constructs, where the 1st, 2nd and both NF-κB sites respectively, were replaced. In each case, the *Xho*I restriction site introduced during the replacement of the NF-κB motifs allowed the screening of the constructs by *Xho*I digestion. The sequences of the promoter region of all the constructs were confirmed by sequence analysis.

Dual Luciferase reporter assay

Transfection of DF-1 cells was carried out with Lipofectamine 2000 (Invitrogen) as per manufacturer's protocols. Approximately 3×10^4 DF-1 cells were seeded in each well of a 96-well plate. Each of the reporter and pcDNA3-v-*rel* constructs were co-transfected into DF-1 cells and the luciferase expression was assayed 48 hours later using the Dual-Glo Luciferase Assay System (Promega) following manufacturer's instructions. The relative expression of

316 *renilla* luciferase was determined with the normalised levels of *firefly* luciferase. For each
317 sample, values from four replicates representative of at least two independent experiments
318 were used in the analysis.

319 **Electrophoresis mobility shift assay (EMSAs)**

320 Recombinant full length v-*rel* from pGEX2t-v-*rel* plasmid in BL21 (DE3) induced with 0.5
321 mM isopropyl-b-D-thiogalactopyranoside (IPTG) for 3h was purified by Glutathione
322 Sepharose 4 Fast Flow (GE Healthcare) according to the manufacturer's instructions. EMSAs
323 were performed using gel shift assay system (Promega) according to the manufacturer's
324 instructions. Double-stranded synthetic oligonucleotides were radiolabeled using [$^{\gamma 32}$P] ATP
325 (Amersham) and T4 polynucleotide kinase. For each binding reaction, 3µg of purified protein
326 was incubated with 0.25µg/µl poly[dI-dC] containing 50,000cpm of radiolabelled probes and
327 a 50-fold molar excess of unlabelled competitor oligonucleotide when indicated. DNA-
328 binding reactions were carried out for 30 min at room temperature. Competition experiments
329 were performed by pre-incubation with protein in binding buffer for 10 min, after which
330 labelled probe was added for a further 20-min incubation at room temperature. The DNA-
331 protein complexes were resolved on 6% DNA Retardation Gel (Invitrogen) and detected by
332 autoradiography.

333 **Immunoblotting and Northern blotting**

334 For Western blotting, cells were lysed in protein gel sample buffer (8 M urea, 2% SDS, 10
335 mM Tris/HCl pH 6.8, 0.05% bromophenol blue) and separated on a NuPAGE 4–12% Bis
336 Tris gel (Invitrogen) and transferred onto nitrocellulose membranes using an iBlot gel
337 transfer system (Invitrogen). Western blotting was performed with c-*rel* and v-*rel*-specific
338 HY87 mouse monoclonal antibody (77), followed by anti-mouse IgG–peroxidase conjugate
339 (Sigma-Aldrich). Membranes were developed with an ECL Western blotting analysis system
340 (Amersham). For Northern blot analysis, total RNA was extracted from cultured cells with

miRNeasy Mini Kit (Qiagen), and 20 µg total RNA resolved using a 15% polyacrylamide-1×Tris-borate-EDTA-8 M urea gel was blotted to a GeneScreen Plus membrane (Perkin-Elmer). DNA oligonucleotides with sequences complementary to candidate miRNAs, end-labelled with [γ-^{32}P]ATP (Amersham) using T4 polynucleotide kinase (New England Biolabs), were used as high-specific-activity probes. Hybridization, washing and autoradiography were carried out as previously described (78).

RCAS virus infection

Virus stocks generated from DF-1 cells transfected with RCAS(A)-v-*rel* and RCAS(A)-v-*rel*-EGFP constructs approximately 5 days after transfection, when nearly 100% cells were EGFP positive in the case of the latter construct. For *in vitro* transformation assay, one ml (~10^6 $TCID_{50}$) of RCAS(A)-v-*rel* virus was used to infect 5x10^6 of embryonic splenocytes, and harvested at day 0, 1, 4, 7, 9 and 14 days post infection for mRNA microarray analysis and miR-155 quantitation. EGFP-expressing RCAS(A)-v-*rel*-EGFP-infected MSB-1 and 265L cells were also sorted and examined for v-*rel* and miR-155 expression.

Stem-loop qRT-PCR for miR-155

The expression levels of miR-155 were analysed using the TaqMan MicroRNA Assay System (Applied Biosystems) using 10 ng of total RNA as a template for reverse transcription. Each reverse transcription reaction was performed twice independently, and each reaction was tested by PCR in triplicates. All values were normalized to the expression of the endogenous let-7a, and levels calculated as fold-expression change relative to those from uninfected 265L cells.

Microarray Analysis

Triplicate RNA samples for each of the six time-points (0, 1, 3, 4, 7 and 14 dpi) were analysed using the Affymetrix GeneChip Chicken Genome Array. Expression values were calculated using the Robust Multi-Array Average (RMA) function within the Affy

bioconductor package (79). Affymetrix probes were linked to Ensembl genes using Ensembl (v70) and genes linked to microRNA predicted targets data from the MicroCosm targets database (80)

For the naïve prediction of miRNAs involved in the activation of genes from the mRNA expression data, the following analysis was performed: down-regulated probes at 14 DPI compared to 0 DPI were determined using Limma (35), with a FDR<=0.01 (81) and log fold change <= -1 (two-fold down-regulated). Statistical enrichment of miRNA targets within the down-regulated gene list was calculated using the CORNA package (82). Fisher's exact test was used to calculate p-values for statistical enrichment, and adjusted for multiple testing (81). Heatmaps were drawn in R using the Pearson correlation coefficient as a similarity measure (83).

In order to analyse the behaviour of predicted gga-miR-155 targets, expression data from Affymetrix probes representing genes predicted to be targets of gga-miR-155 were extracted and analysed as a set.

Funding information

This project was supported by the Biotechnology and Biological Sciences Research Council (BBSRC) grants BB/J004243/1, BB/J004235/1, BB/I01361X/1 and BB/I014284/1 and the State Key Laboratory of Veterinary Biotechnology Foundation (SKLVBF201605).

Acknowledgements

We thank Radmila Hrdlickova, Henry Bose Jr. and Tom Gilmore for kindly providing v-rel reagents.

Conflict of interest

The authors declare no conflict of interest.

Ethics statement

No animals were used for the work presented in this manuscript.

References

1. Gilmore TD, Wolenski FS. NF-kappaB: where did it come from and why? Immunological reviews. 2012;246(1):14-35.
2. Gilmore TD, Gelinas C. Methods for assessing the in vitro transforming activity of NF-kappaB transcription factor c-Rel and related proteins. Methods Mol Biol. 2015;1280:427-46.
3. Robinson FR, Twiehaus MJ. Isolation of tha avian reticuloendothelial virus (strain T). Avian Dis. 1974;18(2):278-88.
4. Hunter JE, Leslie J, Perkins ND. c-Rel and its many roles in cancer: an old story with new twists. Br J Cancer. 2016;114(1):1-6.
5. Chen IS, Mak TW, O'Rear JJ, Temin HM. Characterization of reticuloendotheliosis virus strain T DNA and isolation of a novel variant of reticuloendotheliosis virus strain T by molecular cloning. J Virol. 1981;40(3):800-11.
6. Stephens RM, Rice NR, Hiebsch RR, Bose HR, Jr., Gilden RV. Nucleotide sequence of v-rel: the oncogene of reticuloendotheliosis virus. Proc Natl Acad Sci U S A. 1983;80(20):6229-33.
7. Wilhelmsen KC, Eggleton K, Temin HM. Nucleic acid sequences of the oncogene v-rel in reticuloendotheliosis virus strain T and its cellular homolog, the proto-oncogene c-rel. J Virol. 1984;52(1):172-82.
8. Bose HR, Jr. The Rel family: models for transcriptional regulation and oncogenic transformation. Biochim Biophys Acta. 1992;1114(1):1-17.
9. Gilmore TD, Kalaitzidis D, Liang MC, Starczynowski DT. The c-Rel transcription factor and B-cell proliferation: a deal with the devil. Oncogene. 2004;23(13):2275-86.
10. Sachdev S, Diehl JA, McKinsey TA, Hans A, Hannink M. A threshold nuclear level of the v-Rel oncoprotein is required for transformation of avian lymphocytes. Oncogene. 1997;14(21):2585-94.
11. Kralova J, Liss AS, Bargmann W, Bose HR, Jr. AP-1 factors play an important role in transformation induced by the v-rel oncogene. Mol Cell Biol. 1998;18(5):2997-3009.
12. Liss AS, Tiwari R, Kralova J, Bose HR, Jr. Cell transformation by v-Rel reveals distinct roles of AP-1 family members in Rel/NF-kappaB oncogenesis. Oncogene. 2010;29(35):4925-37.
13. Hrdlickova R, Nehyba J, Bose HR, Jr. Interferon regulatory factor 4 contributes to transformation of v-Rel-expressing fibroblasts. Mol Cell Biol. 2001;21(19):6369-86.
14. Majid SM, Liss AS, You M, Bose HR. The suppression of SH3BGRL is important for v-Rel-mediated transformation. Oncogene. 2006;25(5):756-68.
15. Tiwari R, Bargmann W, Bose HR, Jr. Activation of the TGF-beta/Smad signaling pathway in oncogenic transformation by v-Rel. Virology. 2011;413(1):60-71.
16. Hrdlickova R, Nehyba J, Liss AS, Bose HR, Jr. Mechanism of telomerase activation by v-Rel and its contribution to transformation. J Virol. 2006;80(1):281-95.
17. Gupta N, Delrow J, Drawid A, Sengupta AM, Fan G, Gelinas C. Repression of B-cell linker (BLNK) and B-cell adaptor for phosphoinositide 3-kinase (BCAP) is important for lymphocyte transformation by rel proteins. Cancer Res. 2008;68(3):808-14.

18. Dutta J, Fan G, Gelinas C. CAPERalpha is a novel Rel-TAD-interacting factor that inhibits lymphocyte transformation by the potent Rel/NF-kappaB oncoprotein v-Rel. J Virol. 2008;82(21):10792-802.
19. Hwang HW, Mendell JT. MicroRNAs in cell proliferation, cell death, and tumorigenesis. Br J Cancer. 2006;94(6):776-80.
20. Miska EA. How microRNAs control cell division, differentiation and death. Curr Opin Genet Dev. 2005;15(5):563-8.
21. Wienholds E, Kloosterman WP, Miska E, Alvarez-Saavedra E, Berezikov E, de Bruijn E, et al. MicroRNA expression in zebrafish embryonic development. Science. 2005;309(5732):310-1.
22. Calame K. MicroRNA-155 function in B Cells. Immunity. 2007;27(6):825-7.
23. Teng G, Papavasiliou FN. Shhh! Silencing by microRNA-155. Philos Trans R Soc Lond B Biol Sci. 2009;364(1517):631-7.
24. Mashima R. Physiological roles of miR-155. Immunology. 2015;145(3):323-33.
25. Vigorito E, Kohlhaas S, Lu D, Leyland R. miR-155: an ancient regulator of the immune system. Immunol Rev. 2013;253(1):146-57.
26. Clurman BE, Hayward WS. Multiple proto-oncogene activations in avian leukosis virus-induced lymphomas: evidence for stage-specific events. Mol Cell Biol. 1989;9(6):2657-64.
27. Tam W, Hughes SH, Hayward WS, Besmer P. Avian bic, a gene isolated from a common retroviral site in avian leukosis virus-induced lymphomas that encodes a noncoding RNA, cooperates with c-myc in lymphomagenesis and erythroleukemogenesis. J Virol. 2002;76(9):4275-86.
28. Huskova H, Korecka K, Karban J, Vargova J, Vargova K, Dusilkova N, et al. Oncogenic microRNA-155 and its target PU.1: an integrative gene expression study in six of the most prevalent lymphomas. Int J Hematol. 2015;102(4):441-50.
29. Justice Jt, Malhotra S, Ruano M, Li Y, Zavala G, Lee N, et al. The MET gene is a common integration target in avian leukosis virus subgroup J-induced chicken hemangiomas. J Virol. 2015;89(9):4712-9.
30. Salemi D, Cammarata G, Agueli C, Augugliaro L, Corrado C, Bica MG, et al. miR-155 regulative network in FLT3 mutated acute myeloid leukemia. Leuk Res. 2015;39(8):883-96.
31. Miao J, Bao Y, Ye J, Shao H, Qian K, Qin A. Transcriptional Profiling of Host Gene Expression in Chicken Embryo Fibroblasts Infected with Reticuloendotheliosis Virus Strain HA1101. PLoS One. 2015;10(5):e0126992.
32. Yao Y, Zhao Y, Smith LP, Lawrie CH, Saunders NJ, Watson M, et al. Differential expression of microRNAs in Marek's disease virus-transformed T-lymphoma cell lines. J Gen Virol. 2009;90(Pt 7):1551-9.
33. Bolisetty MT, Dy G, Tam W, Beemon KL. Reticuloendotheliosis virus strain T induces miR-155, which targets JARID2 and promotes cell survival. J Virol. 2009;83(23):12009-17.
34. Heinemeyer T, Wingender E, Reuter I, Hermjakob H, Kel AE, Kel OV, et al. Databases on transcriptional regulation: TRANSFAC, TRRD and COMPEL. Nucleic Acids Res. 1998;26(1):362-7.
35. Smyth GK. Limma: linear models for microarray data. In: Gentleman R, Carey V, Dudoit S, Irizarry R, Huber W, editors. Bioinformatics and Computational Biology Solutions using R and Bioconductor. New York: Springer; 2005. p. 397-420.
36. Costinean S, Zanesi N, Pekarsky Y, Tili E, Volinia S, Heerema N, et al. Pre-B cell proliferation and lymphoblastic leukemia/high-grade lymphoma in E(mu)-miR155 transgenic mice. Proc Natl Acad Sci U S A. 2006;103(18):7024-9.

37. Eis PS, Tam W, Sun L, Chadburn A, Li Z, Gomez MF, et al. Accumulation of miR-155 and BIC RNA in human B cell lymphomas. Proc Natl Acad Sci U S A. 2005;102(10):3627-32.
38. Lawrie CH, Soneji S, Marafioti T, Cooper CD, Palazzo S, Paterson JC, et al. MicroRNA expression distinguishes between germinal center B cell-like and activated B cell-like subtypes of diffuse large B cell lymphoma. Int J Cancer. 2007;121(5):1156-61.
39. van den Berg A, Kroesen BJ, Kooistra K, de Jong D, Briggs J, Blokzijl T, et al. High expression of B-cell receptor inducible gene BIC in all subtypes of Hodgkin lymphoma. Genes Chromosomes Cancer. 2003;37(1):20-8.
40. Yin Q, McBride J, Fewell C, Lacey M, Wang X, Lin Z, et al. MicroRNA-155 is an Epstein-Barr virus-induced gene that modulates Epstein-Barr virus-regulated gene expression pathways. J Virol. 2008;82(11):5295-306.
41. Tam W, Dahlberg JE. miR-155/BIC as an oncogenic microRNA. Genes Chromosomes Cancer. 2006;45(2):211-2.
42. O'Connell RM, Taganov KD, Boldin MP, Cheng G, Baltimore D. MicroRNA-155 is induced during the macrophage inflammatory response. Proc Natl Acad Sci U S A. 2007;104(5):1604-9.
43. Rodriguez A, Vigorito E, Clare S, Warren MV, Couttet P, Soond DR, et al. Requirement of bic/microRNA-155 for normal immune function. Science. 2007;316(5824):608-11.
44. Taganov KD, Boldin MP, Baltimore D. MicroRNAs and immunity: tiny players in a big field. Immunity. 2007;26(2):133-7.
45. Thai TH, Calado DP, Casola S, Ansel KM, Xiao C, Xue Y, et al. Regulation of the germinal center response by microRNA-155. Science. 2007;316(5824):604-8.
46. Yin Q, Wang X, McBride J, Fewell C, Flemington E. B-cell receptor activation induces BIC/miR-155 expression through a conserved AP-1 element. J Biol Chem. 2008;283(5):2654-62.
47. Kong W, Yang H, He L, Zhao JJ, Coppola D, Dalton WS, et al. MicroRNA-155 is regulated by the transforming growth factor beta/Smad pathway and contributes to epithelial cell plasticity by targeting RhoA. Mol Cell Biol. 2008;28(22):6773-84.
48. Gatto G, Rossi A, Rossi D, Kroening S, Bonatti S, Mallardo M. Epstein-Barr virus latent membrane protein 1 trans-activates miR-155 transcription through the NF-{kappa}B pathway. Nucleic Acids Res. 2008.
49. Lu F, Weidmer A, Liu CG, Volinia S, Croce CM, Lieberman PM. Epstein-Barr virus-induced miR-155 attenuates NF-kappaB signaling and stabilizes latent virus persistence. J Virol. 2008;82(21):10436-43.
50. Jiang J, Lee EJ, Schmittgen TD. Increased expression of microRNA-155 in Epstein-Barr virus transformed lymphoblastoid cell lines. Genes Chromosomes Cancer. 2006;45(1):103-6.
51. Kluiver J, Haralambieva E, de Jong D, Blokzijl T, Jacobs S, Kroesen BJ, et al. Lack of BIC and microRNA miR-155 expression in primary cases of Burkitt lymphoma. Genes Chromosomes Cancer. 2006;45(2):147-53.
52. Yao Y, Zhao Y, Xu H, Smith LP, Lawrie CH, Watson M, et al. MicroRNA profile of Marek's disease virus-transformed T-cell line MSB-1: predominance of virus-encoded microRNAs. J Virol. 2008;82(8):4007-15.
53. Zhao Y, Yao Y, Xu H, Lambeth L, Smith LP, Kgosana L, et al. A functional MicroRNA-155 ortholog encoded by the oncogenic Marek's disease virus. J Virol. 2009;83(1):489-92.

54. Wozniakowski G, Mamczur A, Samorek-Salamonowicz E. Common occurrence of Gallid herpesvirus-2 with reticuloendotheliosis virus in chickens caused by possible contamination of vaccine stocks. J Appl Microbiol. 2015;118(4):803-8.
55. Wozniakowski G, Samorek-Salamonowicz E, Kozdrun W. Molecular characteristics of Polish field strains of Marek's disease herpesvirus isolated from vaccinated chickens. Acta veterinaria Scandinavica. 2011;53:10.
56. Sun AJ, Xu XY, Petherbridge L, Zhao YG, Nair V, Cui ZZ. Functional evaluation of the role of reticuloendotheliosis virus long terminal repeat (LTR) integrated into the genome of a field strain of Marek's disease virus. Virology. 2010;397(2):270-6.
57. Dorsett Y, McBride KM, Jankovic M, Gazumyan A, Thai TH, Robbiani DF, et al. MicroRNA-155 suppresses activation-induced cytidine deaminase-mediated Myc-Igh translocation. Immunity. 2008;28(5):630-8.
58. Teng G, Hakimpour P, Landgraf P, Rice A, Tuschl T, Casellas R, et al. MicroRNA-155 is a negative regulator of activation-induced cytidine deaminase. Immunity. 2008;28(5):621-9.
59. Vigorito E, Perks KL, Abreu-Goodger C, Bunting S, Xiang Z, Kohlhaas S, et al. microRNA-155 regulates the generation of immunoglobulin class-switched plasma cells. Immunity. 2007;27(6):847-59.
60. Lu LF, Thai TH, Calado DP, Chaudhry A, Kubo M, Tanaka K, et al. Foxp3-dependent microRNA155 confers competitive fitness to regulatory T cells by targeting SOCS1 protein. Immunity. 2009;30(1):80-91.
61. Ceppi M, Pereira PM, Dunand-Sauthier I, Barras E, Reith W, Santos MA, et al. MicroRNA-155 modulates the interleukin-1 signaling pathway in activated human monocyte-derived dendritic cells. Proc Natl Acad Sci U S A. 2009;106(8):2735-40.
62. Tili E, Michaille JJ, Cimino A, Costinean S, Dumitru CD, Adair B, et al. Modulation of miR-155 and miR-125b levels following lipopolysaccharide/TNF-alpha stimulation and their possible roles in regulating the response to endotoxin shock. J Immunol. 2007;179(8):5082-9.
63. Romania P, Lulli V, Pelosi E, Biffoni M, Peschle C, Marziali G. MicroRNA 155 modulates megakaryopoiesis at progenitor and precursor level by targeting Ets-1 and Meis1 transcription factors. Br J Haematol. 2008;143(4):570-80.
64. Costinean S, Sandhu SK, Pedersen IM, Tili E, Trotta R, Perrotti D, et al. Src homology 2 domain-containing inositol-5-phosphatase and CCAAT enhancer-binding protein beta are targeted by miR-155 in B cells of Emicro-MiR-155 transgenic mice. Blood. 2009;114(7):1374-82.
65. O'Connell RM, Chaudhuri AA, Rao DS, Baltimore D. Inositol phosphatase SHIP1 is a primary target of miR-155. Proc Natl Acad Sci U S A. 2009;106(17):7113-8.
66. Liu WH, Kang SG, Huang Z, Wu CJ, Jin HY, Maine CJ, et al. A miR-155-Peli1-c-Rel pathway controls the generation and function of T follicular helper cells. The Journal of experimental medicine. 2016;213(9):1901-19.
67. Gironella M, Seux M, Xie MJ, Cano C, Tomasini R, Gommeaux J, et al. Tumor protein 53-induced nuclear protein 1 expression is repressed by miR-155, and its restoration inhibits pancreatic tumor development. Proc Natl Acad Sci U S A. 2007;104(41):16170-5.
68. Yang J, Zhang P, Krishna S, Wang J, Lin X, Huang H, et al. Unexpected positive control of NFkappaB and miR-155 by DGKalpha and zeta ensures effector and memory CD8+ T cell differentiation. Oncotarget. 2016;7(23):33744-64.
69. Hayashita Y, Osada H, Tatematsu Y, Yamada H, Yanagisawa K, Tomida S, et al. A polycistronic microRNA cluster, miR-17-92, is overexpressed in human lung cancers and enhances cell proliferation. Cancer research. 2005;65(21):9628-32.

70. Mu P, Han YC, Betel D, Yao E, Squatrito M, Ogrodowski P, et al. Genetic dissection of the miR-17~92 cluster of microRNAs in Myc-induced B-cell lymphomas. Genes & development. 2009;23(24):2806-11.
71. van Haaften G, Agami R. Tumorigenicity of the miR-17-92 cluster distilled. Genes & development. 2010;24(1):1-4.
72. Olive V, Jiang I, He L. mir-17-92, a cluster of miRNAs in the midst of the cancer network. The international journal of biochemistry & cell biology. 2010;42(8):1348-54.
73. Nazerian K. An updated list of avian cell lines and transplantable tumours. Avian Pathol. 1987;16(3):527-44.
74. Akiyama Y, Kato S. Two cell lines from lymphomas of Marek's disease. Biken J. 1974;17(3):105-16.
75. Himly M, Foster DN, Bottoli I, Iacovoni JS, Vogt PK. The DF-1 chicken fibroblast cell line: transformation induced by diverse oncogenes and cell death resulting from infection by avian leukosis viruses. Virology. 1998;248(2):295-304.
76. Hughes SH. The RCAS vector system. Folia biologica. 2004;50(3-4):107-19.
77. Hrdlickova R, Nehyba J, Humphries EH. v-rel induces expression of three avian immunoregulatory surface receptors more efficiently than c-rel. J Virol. 1994;68(1):308-19.
78. Yao Y, Zhao Y, Xu H, Smith LP, Lawrie CH, Sewer A, et al. Marek's disease virus type 2 (MDV-2)-encoded microRNAs show no sequence conservation with those encoded by MDV-1. J Virol. 2007;81(13):7164-70.
79. Gautier L, Cope L, Bolstad BM, Irizarry RA. affy--analysis of Affymetrix GeneChip data at the probe level. Bioinformatics. 2004;20(3):307-15.
80. Griffiths-Jones S, Saini HK, van Dongen S, Enright AJ. miRBase: tools for microRNA genomics. Nucleic acids research. 2008;36(Database issue):D154-8.
81. Benjamini Y, Hochberg Y. Controlling the false discovery rate: a practical and powerful approach to multiple testing. Journal of the Royal Statistical Society Series B. 1995;57:289-300.
82. Wu X, Watson M. CORNA: testing gene lists for regulation by microRNAs. Bioinformatics. 2009;25(6):832-3.
83. Team RC. R: A language and environment for statistical computing. R Foundation for Statistical Computing. Vienna, Austria2014.

614 **Table 1** Top 20 enriched miRNA targets in the list of 1242 downregulated genes

microRNA	Numbers of miRNA target genes in the population			FDR[4]
	Predicted[1]	Expected[2]	Observed[3]	
gga-mir-155	581	45	73	0.002**
gga-mir-9*	504	39	65	0.002**
gga-mir-217	603	46	69	0.033**
gga-mir-19a	648	50	72	0.045**
gga-mir-23b	633	49	70	0.045**
gga-mir-106	685	53	74	0.055
gga-mir-137	570	44	63	0.065
gga-mir-20a	727	56	77	0.065
gga-mir-124b	557	43	61	0.065
gga-mir-190	549	42	60	0.069
gga-mir-19b	629	48	67	0.069
gga-let-7k	623	48	66	0.077
gga-mir-466	806	62	82	0.080
gga-mir-17-5p	732	56	75	0.095
gga-mir-302b	652	50	67	0.114
gga-mir-135a	646	50	66	0.115
gga-mir-29b	692	53	70	0.115
gga-mir-124a	577	44	60	0.115
gga-mir-153	621	48	64	0.115
gga-mir-146b*	490	38	24	0.122

615 [1]Predicted: The total number of genes predicted to be targets of the microRNA in the
616 population; [2]Expected: The number we would expect to see in our sample by random chance
617 based on our sample size; [3]Observed: The number we actually observed; [4]FDR: The
618 Benjamini and Hochberg adjusted p-value from a two-tailed Fisher's exact test. **indicates
619 FDR <= 0.05

620

Figure legends

Figure 1. Northern blotting analysis for determining miR-155 expression. Twenty micrograms of total RNA extracted from the indicated cells was separated on a 15% denaturing polyacrylamide gel, blotted and hybridized with end-labelled antisense oligonucleotide probes to gga-miR-155. Size markers to indicate the positions of the pre-miRNA and the mature miRNA are shown. The cellular U6 small nuclear RNA served as the loading control.

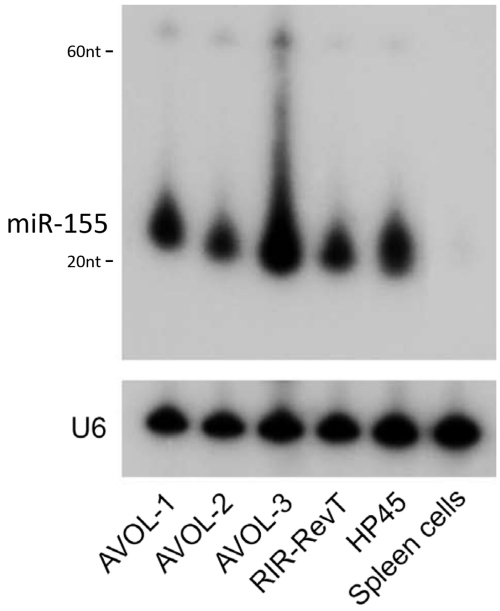

Figure 2. Activation of miR-155 by v-*rel* occurs through the NF-κB pathway. **(A)** Electrophoresis mobility shift assay using purified v-*rel* on the two putative NF-κB binding sites NF-κB1 (−581) and NF-κB2 (−66) on the chicken *Bic*/miR-155 promoter. WT = 50-fold molar cold wild-type competitor, mu = 50-fold molar cold mutant competitor. (**B**) Schematic diagram of luciferase reporter constructs carrying the wild type (WT) and mutant (M1, M2

634 and M1M2) chicken *Bic*/miR-155 promoter. **(C)** Relative levels of luciferase in DF-1 cells
635 co-transfected with pcDNA3-v-*rel* and the reporter constructs. Error bars represent the data
636 from 4 replicates.

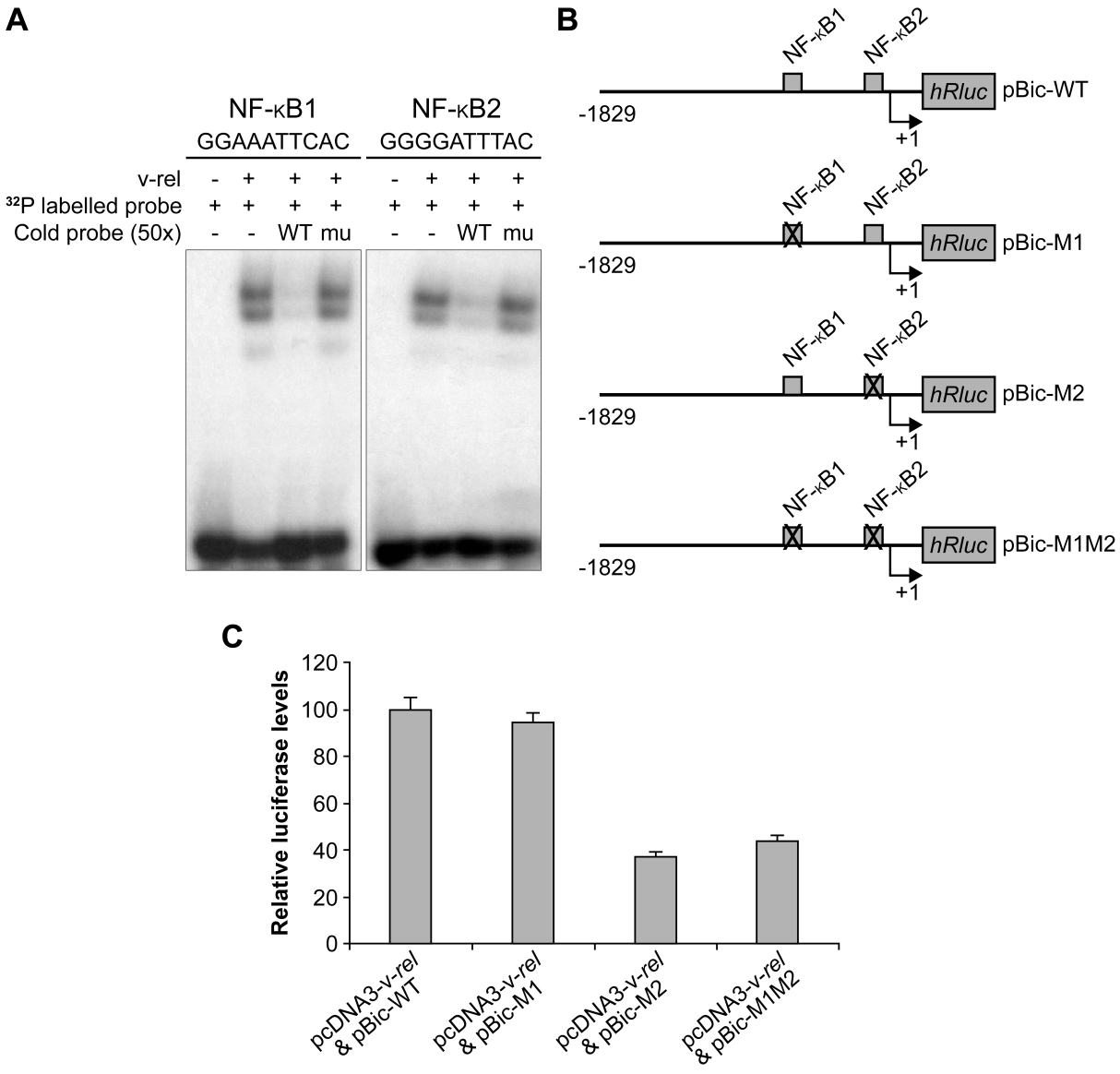

637

638 **Figure 3. Upregulation of miR-155 in MDV-transformed cell lines by v-*rel*. (A)** Cell
639 lysates from MSB-1 and 265L infected with RCAS(A)-v-*rel*-GFP were analysed by Western
640 blot using HY87 antibody for v-*rel* expression. Uninfected MSB-1 and 265L were included
641 as negative control and AVOL-1 cells were included as positive control. **(B)** Expression
642 levels of miR-155 in RCAS(A)-v-*rel*-GFP infected and uninfected MSB-1 and 265L.
643 RCAS(A)-GFP infected cells were also included as a control.

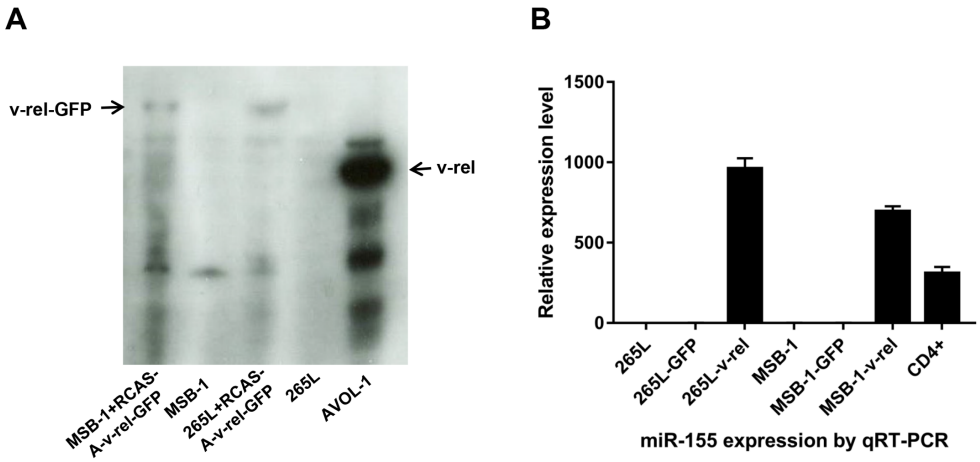

644

645 **Figure 4. Upregulation of miR-155 during v-rel transformation is associated with**
646 **downregulation of targets. (A)** Expression levels of miR-155 in RCAS(A)-v-*rel*
647 transformed embryonic splenocytes on RNA samples harvested on day 0, 1, 4, 7, 9 and 14
648 days post infection. **(B)** Heatmap of 73 down-regulated genes predicted to be targets of gga-
649 miR-155. Affymetrix probes were analysed using Limma, comparing d14 to d0 and those
650 with an FDR<=0.01 and fold-change <= -1 (two-fold) selected. The list was further filtered
651 for those genes predicted to be targeted by gga-miR-155. Heatmap was drawn in R using the
652 Pearson correlation coefficient as a distance measure.

A

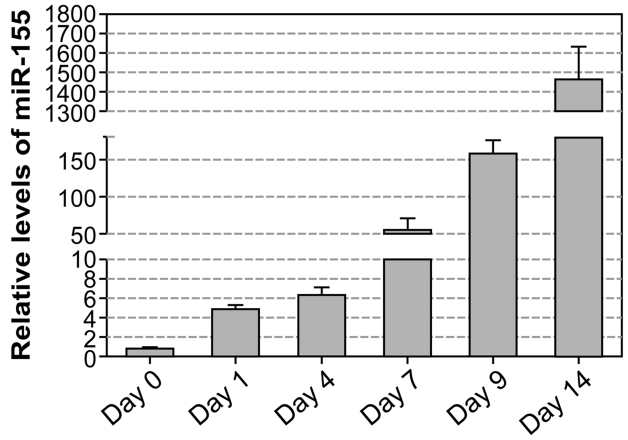
Relative levels of miR-155
1800
1700
1600
1500
1400
1300
150
100
50
10
8
6
4
2
0
Day 0
Day 1
Day 4
Day 7
Day 9
Day 14

B

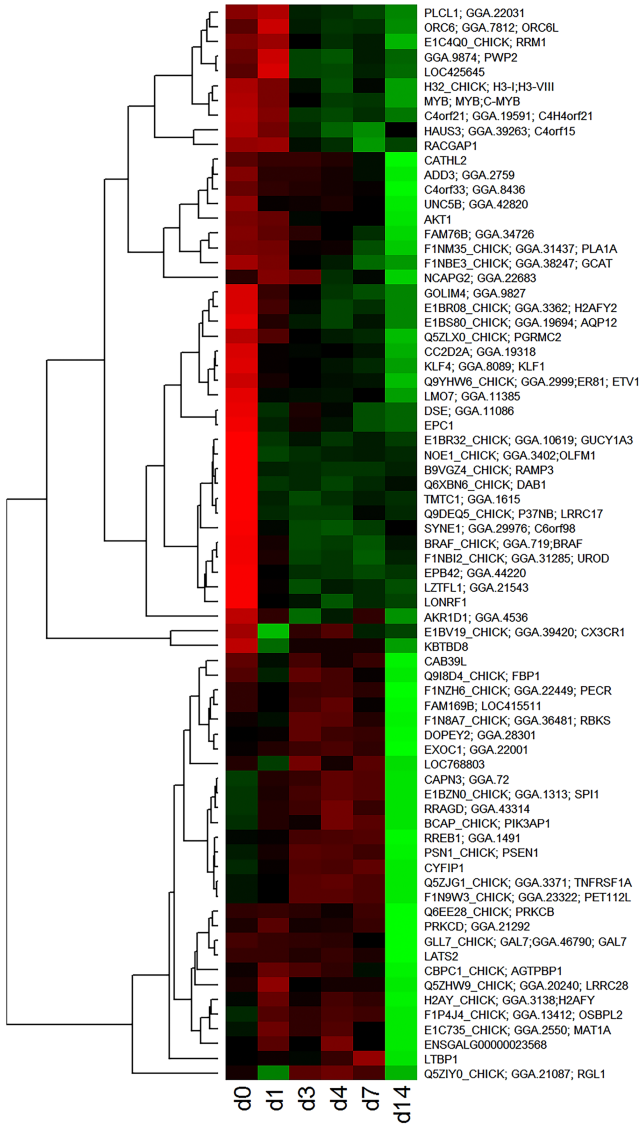
PLCL1; GGA.22031
ORC6; GGA.7812; ORC6L
E1C4Q0_CHICK; RRM1
GGA.9874; PWP2
LOC425645
H32_CHICK; H3-I;H3-VIII
MYB; MYB;C-MYB
C4orf21; GGA.19591; C4H4orf21
HAUS3; GGA.39263; C4orf15
RACGAP1
CATHL2
ADD3; GGA.2759
C4orf33; GGA.8436
UNC5B; GGA.42820
AKT1
FAM76B; GGA.34726
F1NM35_CHICK; GGA.31437; PLA1A
F1NBE3_CHICK; GGA.38247; GCAT
NCAPG2; GGA.22683
GOLIM4; GGA.9827
E1BR08_CHICK; GGA.3362; H2AFY2
E1BS80_CHICK; GGA.19694; AQP12
Q5ZLX0_CHICK; PGRMC2
CC2D2A; GGA.19318
KLF4; GGA.8089; KLF1
Q9YHW6_CHICK; GGA.2999;ER81; ETV1
LMO7; GGA.11385
DSE; GGA.11086
EPC1
E1BR32_CHICK; GGA.10619; GUCY1A3
NOE1_CHICK; GGA.3402;OLFM1
B9VGZ4_CHICK; RAMP3
Q6XBN6_CHICK; DAB1
TMTC1; GGA.1615
Q9DEQ5_CHICK; P37NB; LRRC17
SYNE1; GGA.29976; C6orf98
BRAF_CHICK; GGA.719;BRAF
F1NBI2_CHICK; GGA.31285; UROD
EPB42; GGA.44220
LZTFL1; GGA.21543
LONRF1
AKR1D1; GGA.4536
E1BV19_CHICK; GGA.39420; CX3CR1
KBTBD8
CAB39L
Q9I8D4_CHICK; FBP1
F1NZH6_CHICK; GGA.22449; PECR
FAM169B; LOC415511
F1N8A7_CHICK; GGA.36481; RBKS
DOPEY2; GGA.28301
EXOC1; GGA.22001
LOC768803
CAPN3; GGA.72
E1BZN0_CHICK; GGA.1313; SPI1
RRAGD; GGA.43314
BCAP_CHICK; PIK3AP1
RREB1; GGA.1491
PSN1_CHICK; PSEN1
CYFIP1
Q5ZJG1_CHICK; GGA.3371; TNFRSF1A
F1N9W3_CHICK; GGA.23322; PET112L
Q6EE28_CHICK; PRKCB
PRKCD; GGA.21292
GLL7_CHICK; GAL7;GGA.46790; GAL7
LATS2
CBPC1_CHICK; AGTPBP1
Q5ZHW9_CHICK; GGA.20240; LRRC28
H2AY_CHICK; GGA.3138;H2AFY
F1P4J4_CHICK; GGA.13412; OSBPL2
E1C735_CHICK; GGA.2550; MAT1A
ENSGALG00000023568
LTBP1
Q5ZIY0_CHICK; GGA.21087; RGL1
d0
d1
d3
d4
d7
d14

653

Figure 5. The potential miR-155 targets are involved in a number of dieases and functions. Top 20 functions (sorted by p-value) of the miR-155 targets identified in primary avian macrophages transfected with miR-155 mimics. The grey bars indicate the number of potential target genes for each disease or function.